

Development of a Molecular Recognition Ion Gating Membrane and Estimation of Its Pore Size Control

Taichi Ito, Takanobu Hioki,[†] Takeo Yamaguchi,* Toshio Shinbo,[‡]
Shin-ichi Nakao, and Shoji Kimura[†]

Contribution from the Department of Chemical System Engineering, The University of Tokyo, 7-3-1 Hongo, Bunkyo-ku, 113-8656 Tokyo, Japan, Department of Applied Chemistry, Kogakuin University, 1-24-2 Nishishinjyuku, Shinjyuku-ku, 163-8677 Tokyo, Japan, and National Institute of Advanced Industrial Science and Technology, 1-1 Higashi, Tsukuba 305-8565, Japan

Received December 3, 2001

Abstract: We have fabricated a molecular recognition ion gating membrane. This synthetic membrane spontaneously opens and closes its pores in response to specific solvated ions. In addition to this switching function, we found that this membrane could control its pore size in response to a known concentration of a specific ion. The membrane was prepared by plasma graft copolymerization, which filled the pores of porous polyethylene film with a copolymer of NIPAM (*N*-isopropylacrylamide) and BCAM (benzo[18]crown-6-acrylamide). NIPAM is well-known to have an LCST (lower critical solution temperature), at which its volume changes dramatically in water. The crown receptor of the BCAM traps a specific ion, and causes a shift in the LCST. Therefore, selectively responding to either K⁺ or Ba²⁺, the grafted copolymer swelled and shrank in the pores at a constant temperature between two LCSTs. The solution flux in the absence of Ba²⁺ decreased by about 2 orders of magnitude over a solution flux containing Ba²⁺. The pore size was estimated by the filtration of aqueous dextran solutions with various solute sizes. This revealed that the membrane changed its pore size between 5 and 27 nm in response to the Ba²⁺ concentration changes. No such change was observed for Ca²⁺ solutions. Furthermore, this pore size change occurred uniformly in all pores, as a clear cut-off value for a solute size that could pass through pores was always present. This membrane may be useful not only as a molecular recognition ion gate, but also as a device for spontaneously controlling the permeation flux and solute size.

Introduction

Biomembranes, typified by an ion channel such as a K⁺ channel, can recognize a specific ion, and can control the transport of recognized ions by themselves. This important function maintains the homeostasis of life. Many studies have been conducted on biomimetic membranes that mimic this function. However, there are two problems arising from these studies. The first problem is that the action mechanism of biomembranes is very complicated. The second problem is that many biological substances are easily inactivated by changes in the conditions, such as temperature and pH. Thus, the reappearance of biomembrane functions is very difficult, and the development of a new synthetic biomimetic membrane by other strategies is anticipated. Recently, progress in molecular recognition chemistry has brought about the possibility of designing and synthesizing host compounds, which would have a high degree of molecular recognition, equivalent to the receptors of a biomembrane. Using these host compounds, we may design many synthetic and delicate membrane systems.

Hydrogels change their volume in response to stimulation such as temperature,¹ concentration of ions² and glucose,^{3–5} optical isomers,⁶ antigens,⁷ pH,^{8,9} and light.^{10,11} Using these stimuli-responsive gels, various devices have been suggested. For instance, gating devices that respond to temperature,^{12–14} pH,^{15–17} and glucose concentration¹⁸ have been prepared. In

- (1) Tanaka, T. *Phys. Rev. Lett.* **1978**, *40*, 820–823.
- (2) Irie, M.; Misumi, Y.; Tanaka, T. *Polymer* **1993**, *34*, 4531–4535.
- (3) Kataoka, K.; Miyazaki, H.; Okano, T.; Sakurai, Y. *Macromolecules* **1994**, *27*, 1061–1062.
- (4) Aoki, T.; Nagao, Y.; Sanui, K.; Ogata, N.; Kikuchi, A.; Sakurai, Y.; Kataoka, K.; Okano, T. *Polym. J.* **1996**, *28*, 371–374.
- (5) Kokufuta, E.; Xhang, Y.-Q.; Tanaka, T. *Nature* **1991**, *351*, 302–304.
- (6) Aoki, T.; Muramatsu, M.; Torii, T.; Sanui, K.; Ogata, N. *Macromolecules* **2001**, *34*, 3118–3119.
- (7) Miyata, T.; Asami, N.; Uragami, T. *Nature* **1999**, *399*, 766–769.
- (8) Shigel, R. A.; Firestone, B. A. *Macromolecules* **1988**, *21*, 3254–3259.
- (9) Tatum, T.; Saito, K.; Oyama, N. *Anal. Chem.* **1994**, *66*, 1002–1006.
- (10) Irie, M.; Kungwachakun, P. *Macromolecules* **1986**, *19*, 2476–2480.
- (11) Suzuki, A.; Tanaka, T. *Nature* **1990**, *346*, 345–347.
- (12) Shtanko, N. I.; Kabanov, V. Y.; Apel, P. Y.; Yoshida, M.; Vilenskii, A.-I. *J. Membr. Sci.* **2000**, *179*, 155–161.
- (13) Liang, L.; Shi, M.; Viswanathan, V. V.; Peurrung, L. M.; Young, J. S. J. *J. Membr. Sci.* **2000**, *177*, 97–108.
- (14) Muniz, E. C.; Geuskens, G. *J. Membr. Sci.* **2000**, *172*, 287–293.
- (15) Mika, A. M.; Childs, R. F.; Dickson, J. M.; McCarry, B. E.; Gagnon, D. R. *J. Membr. Sci.* **1995**, *108*, 37–56.
- (16) Mika, A. M.; Childs, R. F. *J. Membr. Sci.* **1999**, *152*, 129–140.
- (17) Winnik, F. M.; Morneau, A.; Mika, A. M.; Childs, R. F.; Roig, A.; Molins, E.; Ziolo, R. F. *Can. J. Chem.* **1998**, *76*, 10–17.
- (18) Ishihara, K.; Kobayashi, M.; Shinohara, I. *Macromol. Chem. Rapid Commun.* **1983**, *4*, 327–331.

* Corresponding author. The University of Tokyo. E-mail: yamag@chemsys.t.u-tokyo.ac.jp.

[†] Kogakuin University.

[‡] National Institute of Advanced Industrial Science and Technology.

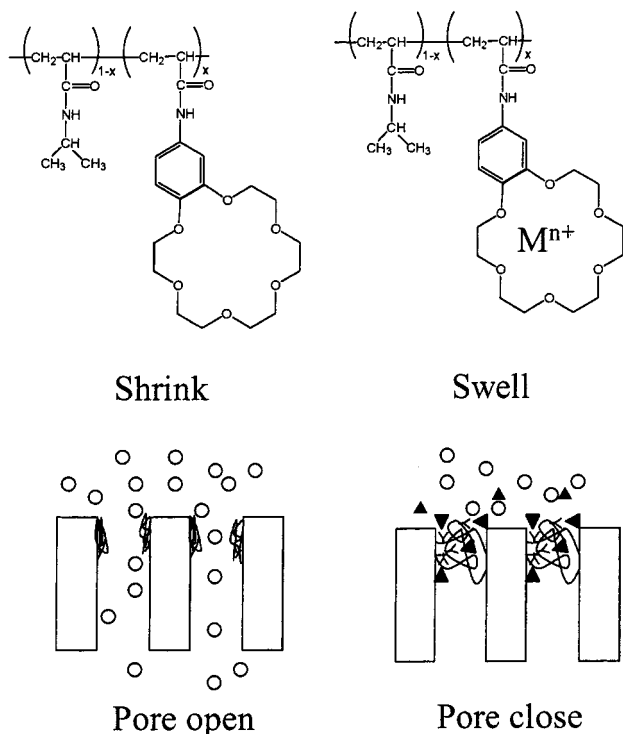


Figure 1. Schematic representation of a molecular recognition ion gating membrane. The copolymer of thermosensitive polymer, NIPAM, and crown ether polymer, BCAM, is grafted on the pore surface. The membrane senses a specific ion, M^{n+} , by the crown ether receptor, and closes its pores rapidly.

these gating systems, there are only a few sensing functions that need to be satisfied by molecular recognition: a response function to control the solution flux at high speed with a high stability.

Ishihara et al.¹⁸ have prepared a glucose gating membrane, which was a fixed grafted copolymer of acrylic acid and GOD (glucose oxidase) in its pores. The solution flux changed to an extent of 10%. Miyata et al.⁷ prepared a hydrogel including both antigens and antibodies. This gel may be used as a gating membrane to control the permeation of hemoglobin in response to rabbit IgGs with response time beyond 1 h. Mika et al. prepared pH valves using poly(acrylic acid)¹⁷ or poly(4-vinylpyridine).¹⁶ A flux change in response to pH was about 3 orders of magnitude. Ito et al. fabricated gating membranes in response to pH,^{19,20} light,²¹ temperature,²² and redox solutions.²³ A water flux of a pH-responsive membrane changed from 2 to 13 g/min by pH change within 3 min. A toluene flux of a light-responsive membrane with spiropyran increased by ultraviolet irradiation and returned by visible light irradiation in a reversible fashion. The change of flux was 6%.

We proposed the concept of a molecular recognition ion gating membrane,²⁴ using synthetic host substances and a thermosensitive polymer. Figure 1 illustrates this concept. This membrane has grafted copolymers of NIPAM (*N*-isopropylacrylamide) and BCAM (benzo[18]crown-6-acrylamide) in its pores. NIPAM is thermosensitive, and the crown ether of BCAM

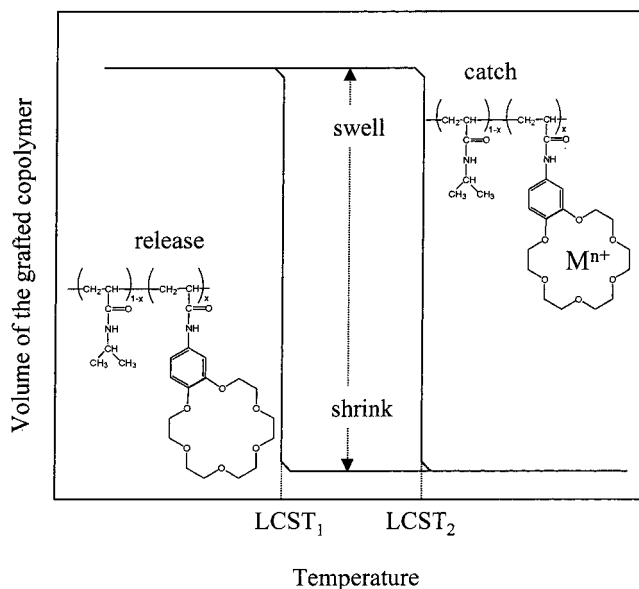


Figure 2. Schematic illustration of the volume change of the grafted NIPAM/BCAM copolymer. On capturing a specific ion, this copolymer changes its LCST from $LCST_1$ to $LCST_2$; thus, the copolymer swells and shrinks in response to M^{n+} at a temperature between $LCST_1$ and $LCST_2$.

selectively traps a specific ion. Therefore, this membrane spontaneously opens and closes its pores by means of the swelling and shrinking of a grafted copolymer in response to a specific ion such as Ba^{2+} or K^+ in solution. At this time, the response behavior was not affected by either Ca^{2+} or Na^+ , as these ions were not captured by the BCAM crown ether receptor. The response speed is below 30 s, because the grafted copolymer is a linear chain.²⁴

The mechanism of molecular recognition response will be explained in more detail. NIPAM has a known LCST (lower critical solution temperature). NIPAM swells below its LCST and shrinks above its LCST, dramatically releasing any free water. The crown ether receptor of BCAM selectively captures a specific ion, the size of which fits the cavity of the BCAM crown ether receptor. As shown in Figure 2, the LCST of the copolymer of NIPAM and BCAM shifts when a specific ion is captured. Consequently, the grafted copolymer swells and shrinks at a temperature located between the two LCSTs in response to Ba^{2+} and K^+ ions. By using the swelling and shrinking actions in the pores, a molecular recognition ion gating membrane can control the solution flux by itself.

In this study, a molecular recognition ion gating membrane was prepared by plasma graft copolymerization and its morphology characterized by FT-IR and environmental scanning electron microscopy (ESEM). In addition, the ability of the membrane to recognize a specific ion and to control its pore size was estimated by the filtration of various aqueous solutions of ions and dextrans. As a result, the molecular recognition ion gating membrane was able to selectively change the solution flux in response to the ions Ba^{2+} , Pb^{2+} , Sr^{2+} , and K^+ independent of other coexisting ions such as Ca^{2+} , Na^+ , and Li^+ . The membrane also changed its pore size between 5 and 27 nm with Ba^{2+} concentration changes. Furthermore, the pore size change occurred uniformly in all pores. However, the membrane did not change its pore size with Ca^{2+} concentration.

Experimental Section

Membrane Preparation. BCAM was synthesized according to reported procedures.^{25,26} Both NIPAM and BCAM were recrystallized

- (19) Park, Y. S.; Ito, Y.; Imanishi, Y. *Chem. Mater.* **1997**, *9*, 2755–2758.
 (20) Ito, Y.; Park, Y. S.; Imanishi, Y. *J. Am. Chem. Soc.* **1997**, *119*, 2739–2740.
 (21) Park, Y. S.; Ito, Y.; Imanishi, Y. *Macromolecules* **1998**, *31*, 2606–2610.
 (22) Park, Y. S.; Ito, Y.; Imanishi, Y. *Langmuir* **1998**, *14*, 910–914.
 (23) Ito, Y.; Nishi, S.; Park, Y. S.; Imanishi, Y. *Macromolecules* **1997**, *30*, 5856–5859.
 (24) Yamaguchi, T.; Ito, T.; Sato, T.; Shinbo, T.; Nakao, S. *J. Am. Chem. Soc.* **1999**, *121*, 4078–4079.

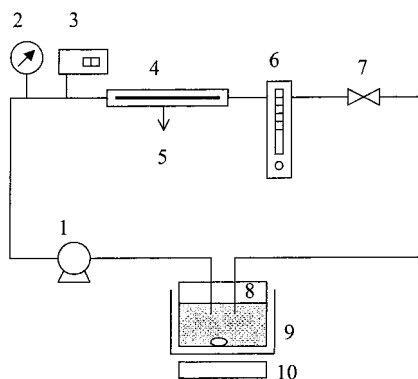


Figure 3. Schematic flow diagram of the filtration experiments. 1. Pump. 2. Pressure gauge. 3. Thermometer. 4. Test cell. 5. Permeation solution. 6. Flow meter. 7. Pressure valve. 8. Feed tank. 9. Thermostat. 10. Stirrer.

from benzene. For monomer solutions, a mixture of NIPAM and BCAM and water was emulsified with SDS (sodium dodecyl sulfate). Both the SDS and the total monomer concentration in solution were fixed at 4 and 5 wt %, respectively. The weight percentage of BCAM in the monomers was varied between 0 and 33 wt %. An HDPE (high-density polyethylene) substrate was used, which was 110 μm thick and had a pore size of 0.2 μm .

Plasma graft copolymerization^{27–29} was used to fix a linear copolymer consisting of NIPAM and BCAM onto the pore surfaces of the membrane. The substrate was irradiated with an argon plasma in order to form initiator radicals, using a plasma power and treatment period of 10 W and 60 s, respectively. After the plasma treatment, two types of graft copolymerization techniques were used: a plasma activation method^{28,29} and a peroxide radical method.²⁷ In the case of the plasma activation method, a monomer solution was introduced by immersing the substrate immediately after the plasma treatment, and was heated to 60 °C. In contrast, in the case of the peroxide radical method, the plasma-treated substrate was in contact with air for 60 s. During this time, the free radicals reacted with O₂ and converted into peroxide radicals. After contacting with the air, a monomer solution was introduced by immersing the treated substrate, and this was heated to 80 °C.

Morphological Analysis. The grafted copolymers formed were measured by FT-IR (Nicolet MAGNA550). The ratio of BCAM to NIPAM in the grafted copolymer was calculated from the ratio of the peak heights at 1388 cm^{-1} , corresponding to the isopropyl group of NIPAM, and 1123 cm^{-1} , corresponding to the ether group of BCAM. The amount of grafting was calculated from the weight.

The change in the pore size was observed with use of ESEM (Nikon ESEM-2700). It can be used to observe wet samples, as the secondary electron detector of the ESEM uses atmospheric gas amplification. The temperature of the membrane was kept at 5 °C, and the relative humidity to the saturated vapor pressure of water was changed from 0 to 100%. This humidity change caused the swelling and shrinking of the grafted copolymer, and thus a change in the pore size could be observed.

Filtration Experiments. Figure 3 shows a schematic diagram of the filtration apparatus. The filtration experiments shown as (1)–(3) below were carried out by cross-flow filtration. A feed solution was flowed parallel to the membrane surface at a flow rate of 500 g/min. The weight percentage of BCAM in the total monomer of the monomer solution used for the preparation of the membrane was 15 wt %, and

Table 1. Weight-Average Molecular Weights and Hydrodynamic Radii of Dextran Samples

sample	M_w [g/mol]	r_s [nm]
T10	10 500	2.7
T40	44 000	5.7
T70	74 000	7.4
T500	470 000	15.3
T2000	1 950 000	27.2

the effective membrane area was 13.2 cm^2 . An applied pressure was maintained at between 0.3 and 0.5 kg f/cm^2 . Instead of the solution flux, the permeability coefficient, L_p , was used to correct for any applied pressure difference and temperature dependence of the solution viscosity. The permeability coefficient was corrected based on the known viscosity of water at 20 °C.

(1) Measurement of the Temperature Dependence of the Solution Flux. Pure water, 0.1 M aqueous LiCl, KCl, NaCl, CaCl₂, BaCl₂, SrCl₂, and PbCl₂, and 0.02 M BaCl₂ solutions were filtrated. The solution temperature was altered from 26 °C to 55 °C. The data of pure water, CaCl₂, and BaCl₂ were taken from our previous paper.²⁴

(2) Measurement of the Ion Concentration Dependence of the Solution Flux. Aqueous NaCl, LiCl, BaCl₂, and PbCl₂ solutions with ion concentrations between 0 and 0.08 M were filtrated. The solution temperature was fixed at 38 °C.

(3) Measurement of the Ion Concentration Dependence and the Rejection Properties. Mixtures of aqueous dextran and BaCl₂ solutions were filtrated. The applied pressure and solution temperature were kept at 1.0 kg f/cm^2 and 38 °C, respectively. The dextran concentration was fixed at 100 ppm, and the BaCl₂ concentration was changed between 0 and 0.014 M. Five different dextrans were used, shown in Table 1. The size of each dextran ranged between 2.7 and 27.2 nm. The dextran size was calculated from the molecular weight by using the Stokes–Einstein and Mark–Houwink relationships as shown by Leburn et al.³⁰

Both the dextran concentration of the feed solution, C_b , and the dextran concentration of the permeate solution, C_p , were measured by using the total organic carbon (TOC) technique (Shimazu TOC-500).³¹ By TOC, dextran in water was burned perfectly and was converted to CO₂, which concentration was measured. The rejection, R , was calculated by using the following definition:

$$R = (C_b - C_p)/C_b$$

Results and Discussion

Difference between the Plasma Activation Method and the Peroxide Radical Method. Membranes were prepared by both plasma activation and peroxide radical copolymerization. The degree of grafting was between 0.3 and 0.5 mg/cm^2 . Figure 4 shows the FT-IR spectra of the membranes prepared by the peroxide radical method. From these spectra, the formation of a grafted copolymer of NIPAM and BCAM was confirmed.

As shown in Figure 5, the ratio of BCAM to NIPAM in the grafted copolymer was much higher by the peroxide radical method than by the plasma activation method. This ratio was estimated from the ratio of the peak heights at 1388 cm^{-1} , from the isopropyl group of NIPAM, and at 1123 cm^{-1} , from the ether group of the BCAM, in the FT-IR spectra.

This difference of copolymer ratio resulted from specificity of the plasma activation method, by which the copolymer ratio of acrylamide and methylacrylate was reported³² to be different from that of ordinary free radical copolymerization. This ratio

(25) Ungaaro, R.; El Haj, B.; Smid, J. *J. Am. Chem. Soc.* **1976**, *98*, 5198–5202.

(26) Yagi, K.; Ruitz, J. A.; Sanchez, M. C. *Macromol. Chem. Rapid Commun.* **1980**, *1*, 263–268.

(27) Suzuki, M.; Kishida, A.; Iwata, H.; Ikada, Y. *Macromolecules* **1986**, *19*, 1804–1808.

(28) Yamaguchi, T.; Nakao, S.; Kimura, S. *Macromolecules* **1991**, *24*, 5522–5527.

(29) Yamaguchi, T.; Nakao, S.; Kimura, S. *J. Polym. Sci., Polym. Chem. Ed.* **1996**, *34*, 1203–1208.

(30) Leburn, L.; Junter, G.-A. *J. Membr. Sci.* **1994**, *88*, 253–261.

(31) Nakao, S.; Kimura, S. *J. Chem. Eng. Jpn.* **1981**, *14*, 32–37.

(32) Yamaguchi, T.; Nakao, S.; Kimura, S. *Ind. Eng. Chem. Res.* **1993**, *32*, 848–853.

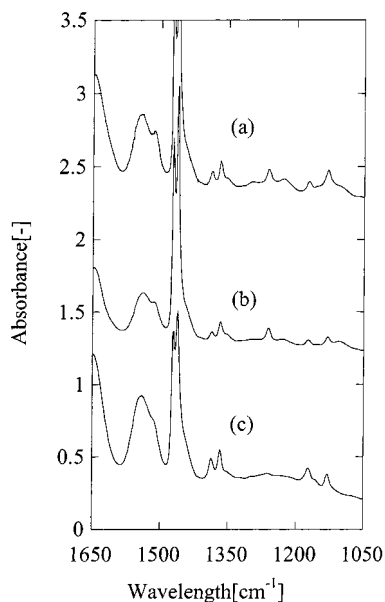


Figure 4. FT-IR spectra of PE-g-NIPAM-co-BCAm prepared by the peroxide plasma graft copolymerization. The weight percentage of BCAM in the total monomer were (a) 15 wt %, (b) 10 wt %, and (c) 5 wt %, respectively.

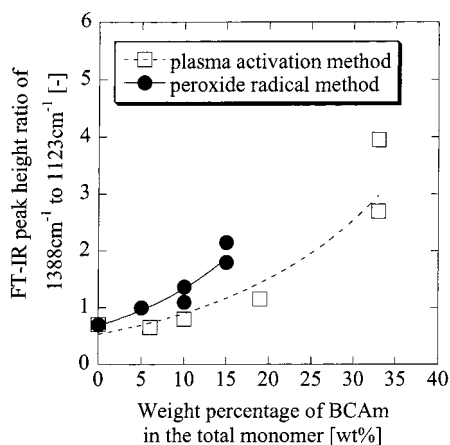


Figure 5. FT-IR peak height ratio of 1388 cm^{-1} to 1123 cm^{-1} of PE-g-NIPAM-co-BCAm. The 1388 cm^{-1} and 1123 cm^{-1} peak represents isopropyl group of NIPAM and ether group of BCAM, respectively. The peroxide radical method grafted more BCAM monomer than the plasma activation method from the same monomer solution.

cannot be explained by the $Q-e$ scheme. On the other hand, in the case of the peroxide method, the argon plasma reacts with oxygen in the air, which then converts into peroxide groups. These peroxide groups are cleaved by heat, and become the initiators of the graft copolymerization. The reaction mechanism of the peroxide radical method was reported^{33,34} to be the same as that of free radical copolymerization. Accordingly, the copolymerization ratio of NIPAM and BCAM was different between the two methods, and thus the BCAM was introduced more efficiently by the peroxide radical method than by the plasma activation method. Therefore, a molecular recognition membrane was prepared by using peroxide plasma graft copolymerization.

(33) Johnson, D. R.; Osada, Y.; Bell, A. T.; Shen, M. *Macromolecules* **1981**, *14*, 118–124.

(34) Paul, C. W.; Bell, A. T.; Soong, D. S. *Macromolecules* **1985**, *18*, 2312–2318.

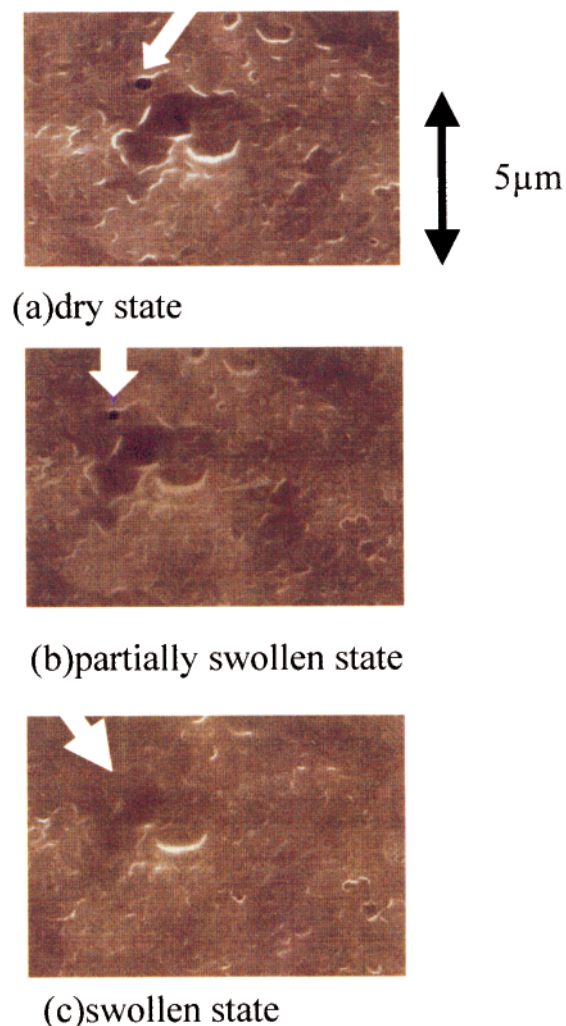


Figure 6. ESEM images of the membrane surface under different humidities. (a) Dry state: relative humidity to the saturated vapor pressure of water was 0%. (b) Partially swollen state. (c) Swollen state: relative humidity was 100%. The arrows show the focused pore. The pore opened and closed in response to humidity change.

Observation of the Opening and the Closure of the Pores. ESEM images of the membrane surface are shown in Figure 6. We focused on a particular pore and observed the change of the pore size under different humidity conditions. Under a dry state, (a), the grafted polymer shrunk and the pore opened. With an increase in the relative humidity (b), the grafted polymer partially swelled and the pore size decreased. Finally, at 100% humidity (c), the pore was perfectly shut.

The composition distribution over a cross-section of a grafted membrane measured with micro FT-IR has been reported.²⁴ From this report, the large quantity of grafted polymer was fixed near to the entrance of the pore, i.e., the designed membrane structure shown in Figure 1 was realized by optimizing the copolymerization conditions.

As a consequence, the pore opened and closed at the entrance of the pore, according to the concept proposed in this study. At the same time, an intermediate state of the pore between the open and closed states was also observed. This is because one side of the grafted polymer was fixed onto the pore surface, while the other side was free. The shrunken grafted polymer was located near the pore surface, and the center of the pore became hollow.

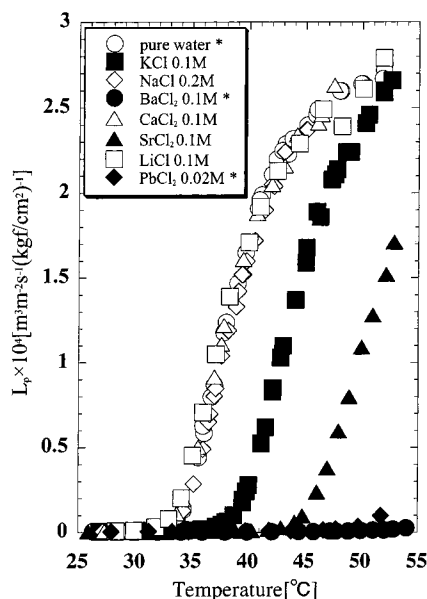


Figure 7. Temperature dependence of the solution permeability coefficient for water containing different ions through the PE-g-NIPAN-co-BCAm. *The data of pure water, Ca^{2+} and Ba^{2+} were taken from our previous paper.

Table 2. Ionic Radii and Formation Constants (K) of Complexes of Benzo[18]crown-6 with Li^+ , Na^+ , K^+ , Ca^{2+} , Sr^{2+} , Pb^{2+} , and Ba^{2+} in Water

ion	ionic radius [Å] ^a	log K [mol ⁻¹ dm ³] ^{b-e}
Li^+	0.76	
Na^+	1.02	1.38
K^+	1.38	1.74
Ca^{2+}	1	0.5
Sr^{2+}	1.18	2.41
Pb^{2+}	1.19	3.19
Ba^{2+}	1.35	2.90

^a Shannon, R. D.; Prewitt, C. T. *Acta Crystallogr., Sect. B* **1969**, 25, 925. ^b Izatt, R. M.; Bradshaw, J. S.; Nielsen, S. A.; Lamb, J. D.; Christensen, J. J.; Seu, D. *Chem. Rev.* **1985**, 85, 271. ^c Katsuta, S.; Tsuchiya, F.; Takeda, Y. *Talanta* **2000**, 51, 637. ^d Takeda, Y.; Kohno, R.; Kudo, Y.; Fukuda, N. *Bull. Chem. Soc. Jpn.* **1989**, 62, 999. ^e $K = [\text{ML}^{m+}]/[\text{M}^{m+}][\text{L}]$; M^{m+} and L are a metal ion and benzo[18]crown-6, respectively.

LCST Shift by Ion Molecular Recognition. Triggered by the capture of ions, the LCST of the membrane, which was defined as a temperature that permeation flux increased from zero, shifted. Figure 7 shows the dependence of the flux of various aqueous ionic solutions on the temperature. The LCST of LiCl, NaCl, and CaCl₂ solutions was 32 °C, similar to that of pure water. In contrast, the LCST of KCl, BaCl₂, SrCl₂, and PbCl₂ solutions were higher than 32 °C (the LCST of pure water). The order of the width of the LCST shift was $\text{Ba}^{2+} > \text{Sr}^{2+} > \text{K}^+ > \text{Li}^+ \approx \text{Na}^+ \approx \text{Ca}^{2+}$ (ignoring Pb^{2+}). The solubility of PbCl₂ was so small that the concentration of PbCl₂ aqueous solution was only 0.02 M.

The order of the complexation constant, log K , of benzo[18]crown-6 in water^{35,36} was $\text{Pb}^{2+} > \text{Ba}^{2+} > \text{Sr}^{2+} > \text{K}^+ > \text{Na}^+ > \text{Ca}^{2+}$, as shown in Table 2. This order shows a good correlation with the order of the LCST shift. In addition, the temperature at the onset of the DSC curve corresponded to LCST of the

membrane.³⁷ From these, we can conclude that molecular recognition by the crown ether receptor caused the shift in LCST.

Smid et al.³⁸ and Maeda et al.^{39–42} measured the complexation properties of poly(vinylbenzo[18]crown-6), vinylbenzo[18]crown-6, BCAM, and poly(BCAM) by picric salt extraction. The amount of extracted ions in the organic solvent layers indicated the complex formation constant (log K) of crown ether. As a result, log K values of poly(vinylbenzo[18]crown-6) and poly(BCAM) were larger than monomer vinylbenzo[18]crown-6 and monomer BCAM, respectively. Poly(BCAM) formed a 2:1 complex, and thus log K of poly(BCAM) was larger than that of monomer BCAM. On the other hand, the monomer BCAM formed a 1:1 complex.

Differing from crown ethers of poly(BCAM), crown receptors of NIPAM/BCAM copolymer form a 1:1 complex and do not form a 2:1 complex, because log K of the crown ether receptor, which was determined³⁷ by impedance measurement, was 1 order of magnitude smaller than that of benzo[18]crown-6 in each cation.

As noted above, log K was small and the ion cation amount captured by crown ether receptors was small. Thus charge repulsion among captured ions was so small that swelling of grafted copolymer does not result from the charge repulsion, but resulted from hydration of formed complexes.³⁷

The change of solution flux began at the LCST, but finished at a temperature that was about 15 °C higher than the LCST. This phenomenon is different from that of poly(NIPAM), and may be the cause of the intermediate state of the pores between the open and closed states.

Control of the Solution Flux by Ion Molecular Recognition. The width of the LCST shift changed in proportion to the concentration of the ion captured by the crown ether receptor. Figure 8 shows the dependence of the flux of 0.01 and 0.10 M aqueous BaCl₂ solutions on the temperature. An increase in BaCl₂ concentration caused an increase in Ba²⁺ ions captured by the crown ether receptor, and a shift in the LCST occurred.

Therefore, an increase in BaCl₂ concentration at a constant temperature caused a phase transition, and the solution flux changed. Figure 9 shows that the solution permeability coefficient solution changed gradually in response to Ba²⁺ concentration changes between 0 and 0.015 M.

ESEM observations showed an intermediate state, where the pores were in neither the fully closed nor the fully opened state. The change in solution flux meant that the pore was stable in this intermediate state. In this way, the membrane acted not only as a molecular recognition ion gate, but also as a device that rapidly and spontaneously controlled the permeation flux by changing its pore size.

Estimation of Pore Size Change by Dextran Aqueous Solution Filtration. The pore size was estimated by filtration experiments on aqueous dextran solutions. Dextrans larger than the pore size are not able to pass through pores, although smaller dextrans may pass through the pores. The rejection, R , quantifies

(37) Ito, T.; Sato, Y.; Yamaguchi, T.; Nakao, S. In preparation.

(38) Kopolow, S.; Hogen Esch, T. E.; Smid, J. *Macromolecules* **1971**, 4, 359–360.

(39) Maeda, T.; Kimura, K.; Shono, T. *Anal. Chem.* **1979**, 298, 363–366.

(40) Kimura, K.; Maeda, T.; Shono, T. *Talanta* **1979**, 26, 945–949.

(41) Kimura, K.; Tsuchida, T.; Maeda, T.; Shono, T. *Talanta* **1980**, 27, 801–805.

(42) Maeda, T.; Kimura, K.; Shono, T. *Anal. Chem.* **1982**, 313, 407–410.

(35) Izatt, R. M.; Bradshaw, J. S.; Nielsen, S. A.; Lamb, J. D.; Christensen, J. J.; Seu, D. *Chem. Rev.* **1985**, 85, 271–339.

(36) Katsuta, S.; Tsuchiya, F.; Takeda, Y. *Talanta* **2000**, 51, 637–644.

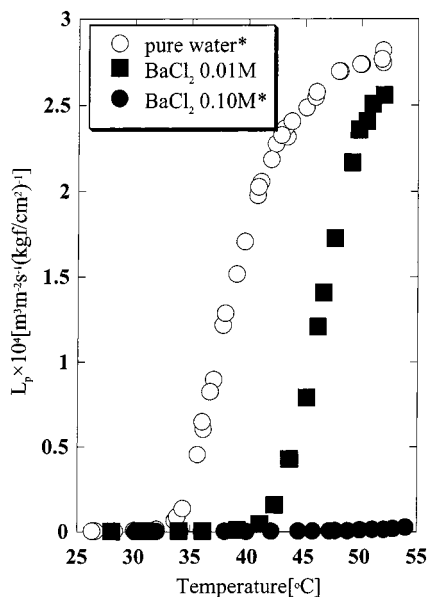


Figure 8. Temperature dependence of the solution permeability coefficient for water containing Ba^{2+} through the PE-g-NIPAN-co-BCAm. *The date of pure water and 0.10M Ba^{2+} were taken from our previous paper.

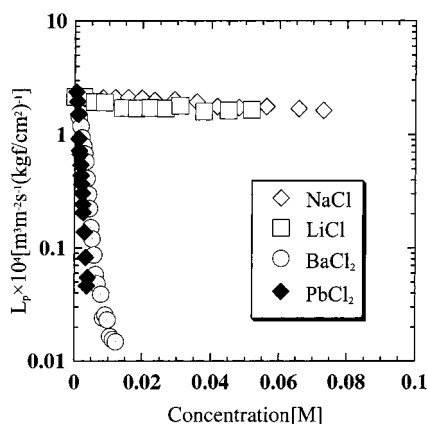


Figure 9. Ion concentration dependence of the solution permeability coefficient for water containing different ions through the PE-g-NIPAN-co-BCAm.

the ratio of rejected dextran to supplied dextran. Accordingly, the pore size was estimated by the cutoff dextran size that had a rejection value of 90%.

Figure 10 shows the relationship between R and the dextran size. The cutoff dextran size was 27.2 nm in the absence of Ba^{2+} , while it decreased to 5.7 nm at a Ba^{2+} concentration of 0.014 M. With increasing Ba^{2+} concentration, this cutoff size gradually decreased, i.e., the pore size decreased.

The rejection, R , was not an indicator of the pore size under high solution flux because of the phenomenon of concentration polarization, where the solute concentration increase on the membrane surface of the feed side is higher than that of the bulk. A high feed concentration and high filtration pressure decrease the diffusivity from the surface to the bulk, and retain the solute on the membrane surface. Thus, the concentration on the membrane surface increases. By this phenomenon, the rejection value seemingly decreases, even though the real rejection of the membrane is high. Figure 11 shows the relationship between the solution size and the flux. The line in Figure 11 is the upper limit of the range where concentration polarization did not occur. All the measurements were performed

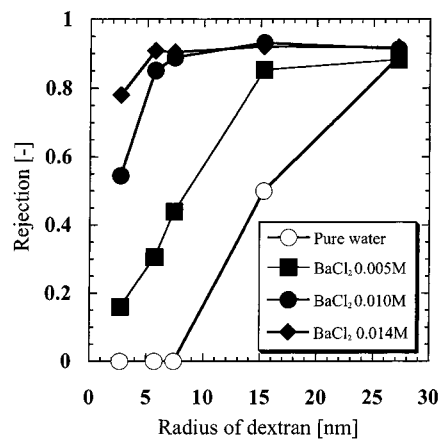


Figure 10. Relationship between the rejection, R , and the dextran radius. The dextran rejection changed in response to Ba^{2+} signal of a different concentration.

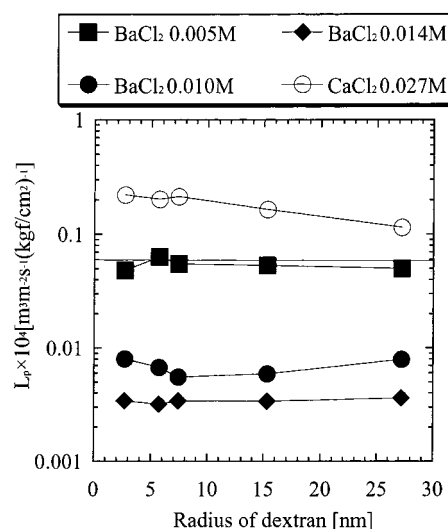


Figure 11. Relationship between L_p and dextran size. Aqueous solutions containing 100 ppm dextran and ions were prepared. The solution temperature, the feed flow rate, and the applied pressure were kept at 38 °C, 500 mL/min, 1.0 kgf/cm², respectively. Under conditions that L_p was below $6 \times 10^{-6} \text{ m}^3 \text{ m}^{-2} \text{ s}^{-1} (\text{kgf/cm}^2)^{-1}$ as shown by the above line, concentration polarization didn't occur, therefore, rejection surely exhibited the relationship between pore sizes and solute sizes.

at values below the upper limit, and therefore the pore size estimated by rejection was appropriate.

In this case, the rejection increased sharply from 0 to 100% for any concentration of Ba^{2+} , and a clear cut-off dextran size was always reached. The pore size distribution was always very narrow, and bore no relationship to change in pore size. The reasons for this are as follows: (i) The NIPAM/BCAm copolymer was homogeneously grafted onto all of the membrane surface area; (ii) the pore size distribution of the porous HDPE substrate was narrow; and (iii) the swelling and shrinking of the grafted polymer occurred simultaneously in all pores.

Compared with the molecular recognition ion gating membrane, the casting membranes of the cross-linked gel also could control the permeability by using its mesh structure. However, as the network of the gel was heterogeneous and the distribution of the mesh size was very wide, the gel membrane could not control the size of the solute.

These functions of sensing and controlling the pore size will help to realize drug delivery systems (DDS), which will release

different drugs in response to specific ion concentrations and will also realize a new separation membrane, which can control rejection in response to a specific ion signal.

Conclusions

We suggested the concept of a molecular recognition ion gating membrane and prepared such a membrane by the peroxide plasma graft copolymerization process. The opening and closing of its pores were observed by ESEM.

A molecular recognition function was investigated by various aqueous ion solution experiments. The order of the width of the LCST shift was observed to be $\text{Ba}^{2+} > \text{Sr}^{2+} > \text{K}^+ > \text{Li}^+ \approx \text{Na}^+ \approx \text{Ca}^{2+}$. This order showed a good correlation with the order of the complexation constant of the crown ether receptor.

Pore size control was investigated by dextran filtration experiments. The membrane spontaneously controlled the solution flux in response to a specific ion such as Ba^{2+} . In addition,

the membrane changed its pore size from 5 to 27 nm in response to a change in Ba^{2+} concentration of between 0 and 0.014 M. The pore size distribution was always very narrow, and bore no relationship to the change in pore size. Therefore, the swelling and the shrinking of the grafted polymer occurred simultaneously in all the pores.

This membrane will probably be used for artificial internal organs, drug delivery systems, and the treatment of wastewater, etc.

Acknowledgment. We gratefully acknowledge T. Sugawara of the University of Tokyo, Japan, for helpful advice and discussion. We also thank the Asahi Chemical Co. Ltd. for supplying the HDPE porous substrate and the Kozin Co. for supplying the NIPAM.

JA012648X